Electroweak results from ATLAS

S. Glazov([1]), on behalf of the ATLAS Collaboration
([1]) *DESY, Notkestrasse 85, 22607, Hamburg, Germany.*

Summary. — Measurements of single W and Z as well as diboson WW, WZ and ZZ production at the LHC performed by the ATLAS collaboration in 2010 and 2011 are presented. The data provide accurate tests of the theory in a wide kinematic range. A QCD analysis of the W and Z boson differential distributions reveals a novel sensitivity to the strange-quark density which is found to be large compared to previous expectations. Studies of $W + b$ and $Z + b$ jet production and W polarisation test NLO QCD calculations and proton PDFs. The diboson cross-section measurements are used to determine limits on the anomalous couplings. No deviation from the Standard Model is observed.

PACS 12.38.Qk,13.38.Be,13.38.Dg,14.70.Hp,12.15Ji,12.60.Cn, 13.85.Qk – 13.85.Qk.

1. – Introduction

Successful start and continues delivery of the luminosity enabled rediscovery of the Standard Model processes at the LHC. The processes with the highest cross section, such as production of single W and Z bosons, were accurately measured already using the data collected during the first year of the operation, in 2010. Further increase of the integrated luminosity in 2011 allowed the ATLAS collaboration to extend the reach to more rare processes, in particular production of diboson states.

The measurements reported by the LHC collaborations have an unprecedented accuracy for the detectors which are at the beginning of their operation cycle. In particular, the ATLAS detector shows very good performance. For example, the lepton (e, μ) identification efficiency is understood typically to better than 1%, the calorimeter energy scale is known to better than 1% [1], and the jet energy scale is calibrated with up to 2.5% accuracy for the central jets at medium transverse momenta (p_T) [2]. Last but not least ingredient enabling success of the Standard Model physics analyses at the LHC is the accurate determination of the luminosity which is measured to 3.4% precision [3].

Standard Model predictions at the LHC require higher order QCD calculations and knowledge of the proton structure. The parton distribution functions (PDFs) are measured primarily using deep-inelastic lepton-proton scattering data. The PDFs are parameterised as a function of Bjorken-x variable, their values at different four momentum

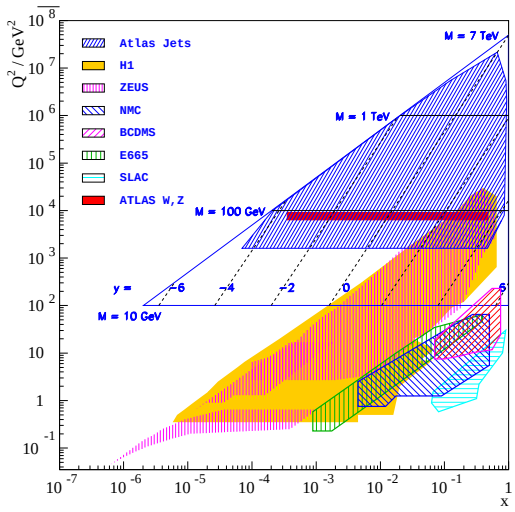

Fig. 1. – Kinematic reach of the measurements at fixed target and collider ep experiments and at the LHC.

transfers Q^2 are related using evolution equations. The pp scattering processes at the LHC are predicted using these universal PDFs and coefficient functions, calculated perturbatively. Large center of mass energy $S = 4E_p^2$ of the LHC leads to a kinematic coverage extending to high Q^2 and low x, see Figure 1. Comparison of the data with the predictions thus provides tests of perturbative QCD and shed additional light on the proton structure.

2. – Measurements based on production of W and Z bosons

The production of W, Z vector bosons at the LHC is the standard candle process which can be used to calibrate and monitor performance of the detectors and to validate the Standard Model predictions. Accurate measurements of the W and Z boson production are performed by the ATLAS collaboration in the electron and muon channels [4] using the data collected in 2010. The Standard Model predicts that W and Z bosons couple identically to the leptons from different generations and thus production rates should be the same up to effects proportional to the lepton masses ("lepton universality"). Figure 2 shows that the ATLAS measurements expressed in term of the ratios of $Z \to e^+e^-$ to $Z \to \mu^+\mu^-$ and $W^\pm \to e\nu$ to $W^\pm \to \mu\nu$ production cross sections are consistent with the lepton universality at a few percent level of accuracy. For the W boson, the precision of the result is comparable the PDG world average [5].

The measurements of the total cross section in e and μ channels are combined and compared to the predictions in Figure 3 which shows experimental results obtained at pp and $p\bar{p}$ colliders and at different center of mass energies. For $p\bar{p}$ colliders, W^+ and W^- production has identical cross section while for pp colliders W^+ production cross section is larger since the u-quark has larger density that the d-quark. Overall, there is a very good agreement between the data and expectations. There is also a very good agreement observed between ATLAS and CMS total cross-section measurements.

Additional information on the proton structure can be obtained by performing differ-

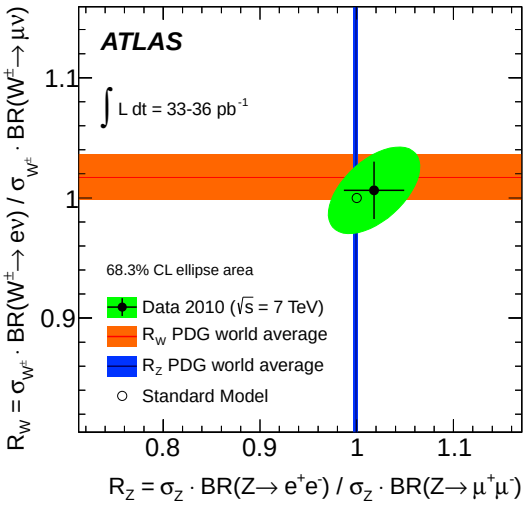

Fig. 2. – ATLAS results for the ratio of cross-section measurements in e and μ channel for Z and W production compared to the PDG and Standard Model expectations [4]. The ellipse shows the 68% CL for the correlated measurement of the ratios while the error bars correspond to the one-dimensional uncertainties.

ential cross-section measurements, in particular by using the boson rapidity y. At leading order, y is given by x_1 and x_2 values of the colliding quarks as $x_{1,2} = M/\sqrt{S}\exp(\pm y)$ where $M = M_W$ or $M = M_Z$. Since for the W bosons it is impossible to reconstruct y due to the missing neutrino, the pseudorapidity of the reconstructed lepton η_ℓ is used instead.

The combined differential cross sections $d\sigma/d\eta_\ell$ and $d\sigma/dy_Z$ were included in a QCD fit [7] using a HERAFitter program [8]. The analysis uses full correlation information among the measurements. Two fits were performed, using different levels of the strange-

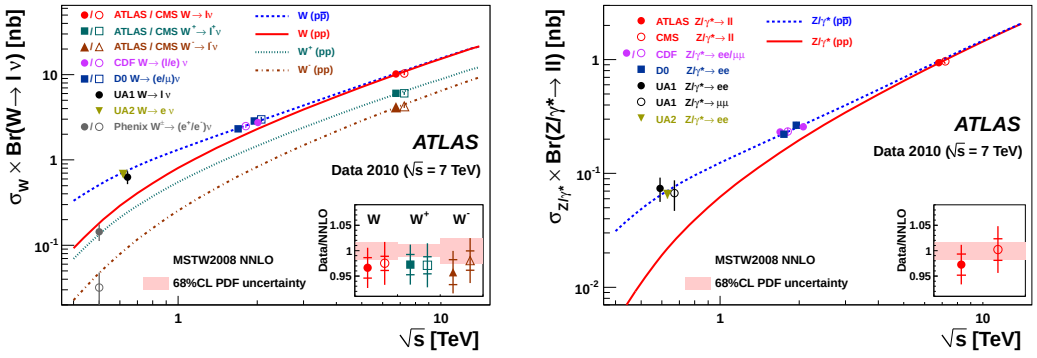

Fig. 3. – Total $W^\pm$ and Z cross section measured at pp and $p\bar{p}$ colliders at different $\sqrt{s}$ [6]. The inserts show the results at $\sqrt{S} = 7$ TeV from the ATLAS and CMS collaborations as ratios to NNLO predictions.

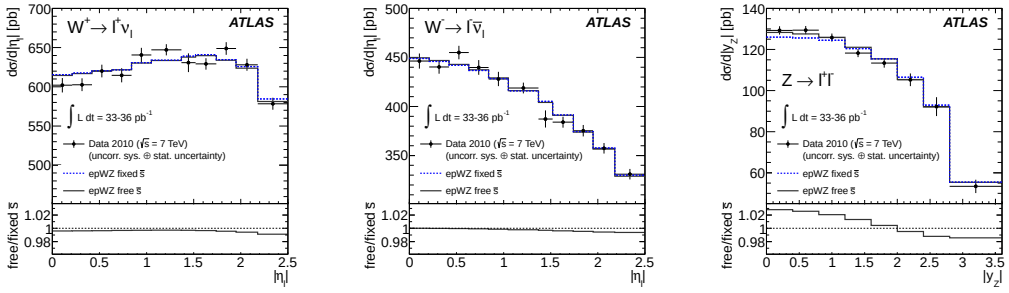

Fig. 4. – Differential $d\sigma/d\eta_\ell$ (left,middle) cross-section measurement for $W \to \ell\nu$ and $d\sigma/d_Z$ (right) cross-section measurement for $Z \to \ell\ell$ [7]. The error bars represent statistical and uncorrelated systematic uncertainties added in quadrature while the theory predictions are adjusted for the correlated systematic error shifts. The fits with free and fixed strangeness are shown, and their ratios are given in the lower panels.

sea quark density, they are shown in Figure 4. The fit in which ratio of strange-to-down quark density $r_s = 0.5(\bar{s}+s)/\bar{d}$ is let free shows significantly improved agreement with the data compared to the fit with fixed $r_s = 0.5$.

The ATLAS measures $r_s = 1.00^{+0.09}_{-0.10}$ at $x = 0.013$, corresponding to $y_Z = 0$, and $Q^2 = M_Z^2$. The measurement is compared in figure 5 with predictions from different PDF groups. The ATLAS data are above all expectations, they are consistent with the prediction of CT10 [9], while the other groups show lower values. The large strangeness fraction results in a better description of the ratio of the W to Z total cross sections, calculated in fiducial volume of the measurement, as it is also shown in the Figure 5.

The flavour decomposition of PDFs can be also studied using boson production with jets where the jets are flavour tagged using displaced vertex information or B-meson decays. The $W + b$-jet production is, however, mostly sensitive to the b-quark production from the QCD radiation. The ATLAS results [11] are shown in Figure 6, they are somewhat exceeding the expectations for larger jet multiplicities, however the data and theory are consistent within the uncertainties. The production of b-tagged jets associated with the Z boson provides a check of the b-quark PDF. Larger coupling to the Z boson for the b compared to c quark can lead to improved sensitivity with respect to the measurements

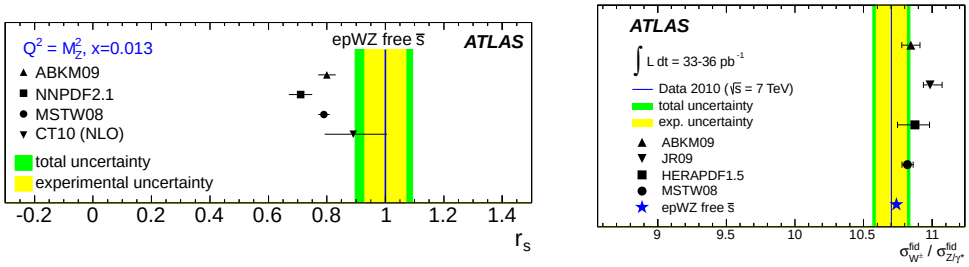

Fig. 5. – Predictions obtained for the ratio r_s at $Q^2 = M_Z$ and $x = 0.013$ (left). Ratio of fiducial cross sections, $(W^+ + W^-)/Z$ (right) [10]. Points show predictions from different PDF groups, bands represent the ATLAS result with inner band showing experimental and outer band total uncertainty. The blue star "epWZ free $\bar{s}$" is the result of the ATLAS fit.

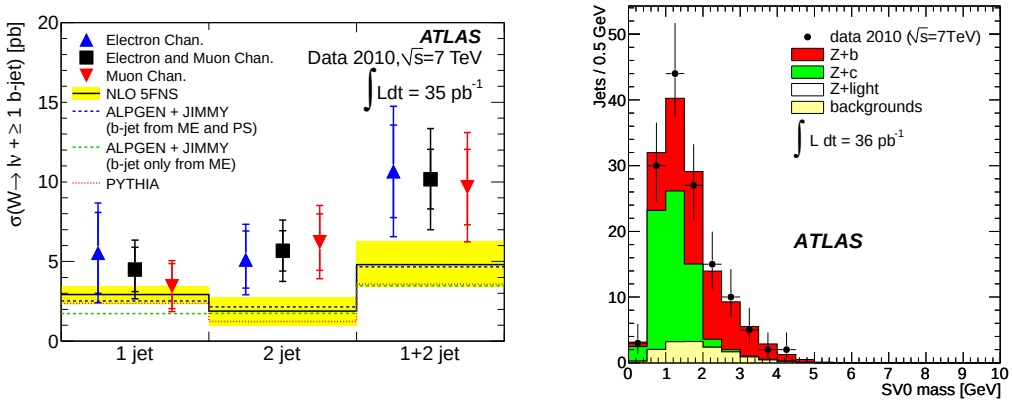

Fig. 6. – Measured fiducial cross section for W and b-jet production in electron, muon and combined electron plus muon channel (left) [11]. The cross section is given in 1, 2, and $1+2$ exclusive bins. The measurements are compared with NLO predictions with total uncertainties, estimated as a sum in quadrature of the renormalisation and factorisation scale variation, PDF and non-perturbative correction uncertainties. Secondary vertex mass distribution for jets in Z and b-tagged jet events (right) [12]. The fitted contributions from b, light, and c-jets are displayed together with other backgrounds.

of the b-PDF at HERA. Figure 6 shows the secondary vertex mass distribution which indicates high purity of $Z+b$ jet events for high masses. The ATLAS result for the $Z+b$ jet production cross section [12] is consistent with the expectations.

At leading order QCD, W bosons are produced left- (f_L) or right-handed (f_R) and for large rapidities they are predominantly left-handed since on average the valence quarks

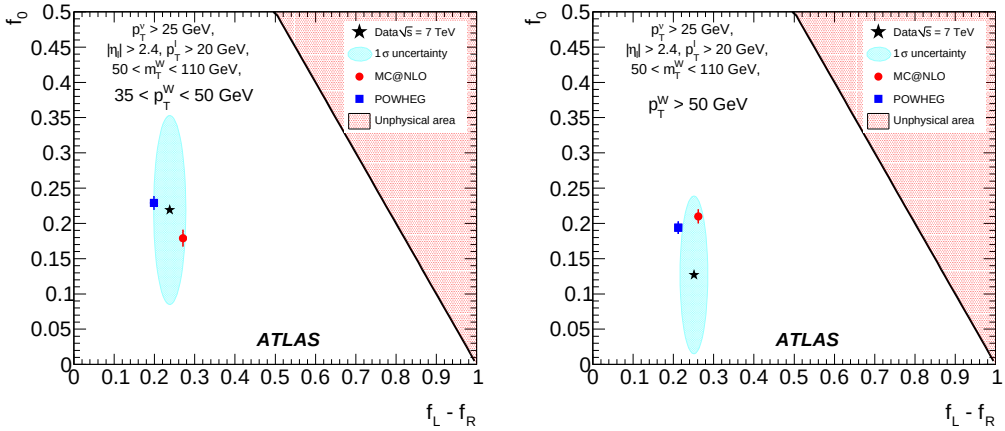

Fig. 7. – Measured values of f_0 and $f_L - f_R$, after corrections, with acceptance cuts for $35 < p_T^W < 50$ GeV (left) and for $p_T^W > 50$ GeV (right) compared with the predictions from NLO simulations [13]. The ellipses around the data points correspond to one standard deviation, summing quadratically the statistical and systematic uncertainties.

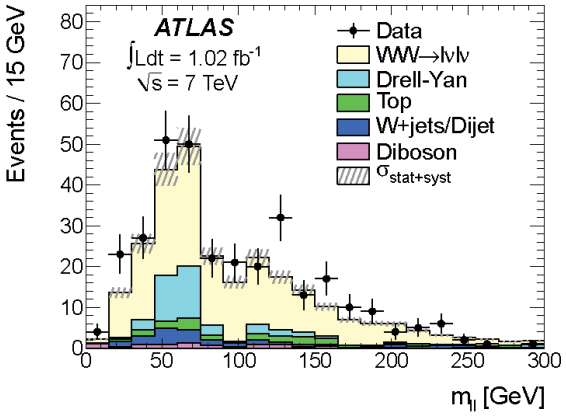

Fig. 8. – The distribution of the invariant mass of the charged leptons after the final selection for WW candidates from combined ee, $\mu\mu$ and $e\mu$ channels [14]. The data (dots) are compared to the expectation from WW and the background contributions.

carry larger momenta compared to the sea antiquarks. A comparison of left- vs right-handed W bosons thus gives a handle on the valence – sea quark separation. In addition, at NLO, for production at significant transverse momentum p_T^W, the longitudinal polarisation (f_0) arises from the gluon density. The polarisation fractions obey $f_L + f_R + f_0 = 1$ relation leaving two of them independent. ATLAS measurements [13] are shown in Figure 7 in terms of f_0 as a function of $f_L - f_R$ for different ranges in p_T^W. The ATLAS result establishes $f_L > f_R$ as expected from the valence quark dominance. The longitudinal polarisation fraction f_0 is consistent with the expectations and is above zero at 1–2σ level.

3. – Measurements of diboson production

At the LHC, the main diagrams for the W^+W^- production are the t-channel quark exchange and the s-channel diagram containing the triple gauge coupling (TGC) vertex. The gluon-gluon fusion box diagram contributes less that 10% at $\sqrt{S} = 7$ TeV. For the ZZ and WZ pair production, the TGC vertex vanishes in the Standard Model. Accurate measurements of the diboson production cross sections provide thus stringent tests of the Standard Model and may show indications of physics beyond it. All ATLAS results presented here are based on 1.02 fb^{-1} of data collected in 2011.

For the processes involving massive gauge bosons in the final state, W^+W^- production has the highest cross section. The final state is however not fully reconstructed and there are sizable background contributions even after all selection criteria are applied, providing additional challenges for the analysis. The ATLAS collaboration measured the W^+W^- production cross section using $\mu^+\mu^-$, e^+e^- and $e^\pm\mu^\mp$ final states with missing transverse energy [14]. The ATLAS measurement, $\sigma(pp \to WW) = 54 \pm 4.0_{\rm stat} \pm 3.9_{\rm syst} \pm 2.0_{\rm lumi}$ pb, is found to be consistent with the Standard Model prediction of 44.4 ± 2.8 pb. Figure 8 shows comparisons of the data with the sum of the signal and background predictions for the invariant mass of the charged leptons. Background contribution from the Drell-Yan process around the Z-boson mass is clearly

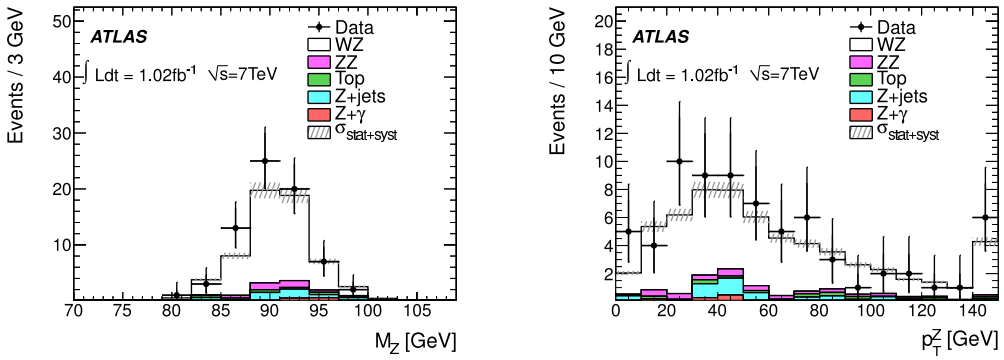

Fig. 9. – For WZ candidates after the full selection, the invariant mass of the lepton pair attributed to the Z boson (left) and the transverse momentum of the Z boson (right) [15]. The stacked histograms represent the predictions from simulation or data-driven estimates, including the uncertainties shown by shaded bands. The last bin of the right panel includes the overflow.

visible in this plot. No significant deviation from the expectation is observed.

Compared to WW production, requirement of a presence of a fully reconstructed Z boson suppresses the background processes for the WZ production. The invariant mass of the lepton pair for the Z boson candidates in shown in Figure 9 where only small contamination of the background is observed. The total cross section measured by ATLAS [15], $\sigma(pp \to WZ) = 20.5^{+3.1}_{-2.8\,\mathrm{stat}}{}^{+1.4}_{-1.3\,\mathrm{syst}}{}^{+0.9}_{-0.8\,\mathrm{lumi}}$ pb, is consistent with the Standard Model prediction $17.3^{+1.3}_{-0.8}$ pb. There is also good agreement observed between the measured transverse momentum distribution of the Z boson and the expectations, up to highest p_T^Z values, see Figure 9.

The ATLAS measurement of ZZ production in $2\mu2\mu$, $2e2e$ and $2\mu2e$ channels [16] is based on observed 12 events with a background expectation of $0.3 \pm 0.3_{\mathrm{stat}}\,^{+0.4}_{-0.3\,\mathrm{syst}}$ events. The correlation of the invariant masses of the dilepton pairs for the leading and sub-leading in p_T Z boson candidates is shown in Figure 10. Based on these data, the ATLAS collaboration measured the production cross section of $\sigma(pp \to ZZ) = 8.5^{+2.7}_{-2.3\,\mathrm{stat}}{}^{+0.4}_{-0.3\,\mathrm{syst}} \pm 0.3_{\mathrm{lumi}}$ pb which is consistent with the Standard Model expectation of $6.5^{+0.3}_{-0.2}$ pb.

From the measurement of the WW, WZ and ZZ diboson production the ATLAS collaboration has derived limits on the anomalous TGC. An example result is shown for the forbidden $Z(\gamma) \to ZZ$ coupling in Figure 10. The limits are comparable to those obtained by the other experiments.

4. – Summary

The ATLAS measurements of the Standard Model processes show remarkable agreement between the data and expectations. The data are precise enough to impose constraints on the proton structure. An accurate measurement of the W and Z production cross sections provides a check of the lepton universality. The differential measurements are used as a stringent test of the proton PDFs; a QCD analysis of the data reveals a novel constraint on the strange-sea quark density which is found to be unsuppressed compared to the down-sea. Studies of $W + b$ and $Z + b$ jet production are used to investigate higher order QCD effects and the b-quark density. The valence and gluon densities are

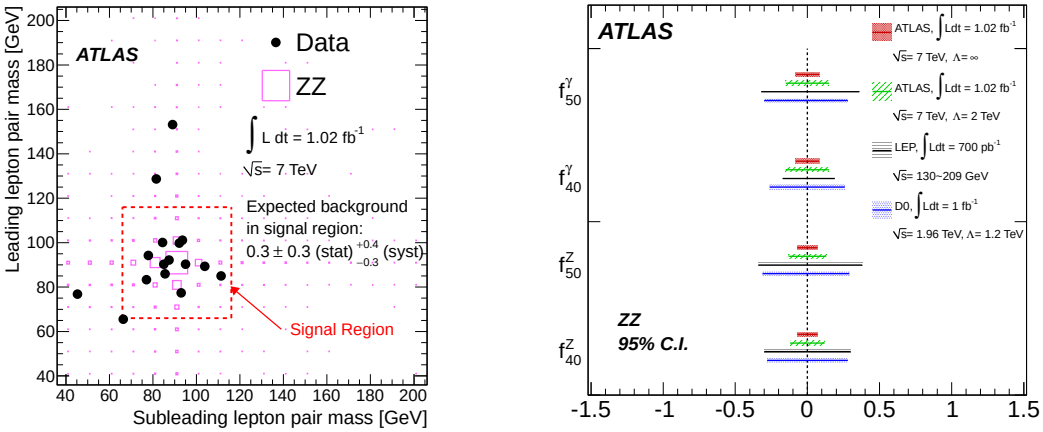

Fig. 10. – The mass of the leading lepton pair versus the mass of the subleading lepton pair for the ZZ candidate events (left) [16]. The events observed in the data are shown as solid circles and the ZZ signal prediction from the simulation as boxes. Anomalous TGC 95% confidence intervals from various experiments (right).

probed using the measurement of the W-polarisation, consistency is observed between the data and NLO QCD calculations.

The data collected in 2011 were used to measure the rare WW, WZ and ZZ diboson production processes. For all of them, the data are found to be consistent with the Standard Model expectations. Limits are derived on the anomalous couplings which are competitive with the other experiments.

REFERENCES

[1] ATLAS Collaboration, *Eur. Phys. J*, **C72** (2012) 1909;
[2] ATLAS Collaboration, arXiv:1203.1302 [hep-ex] (2012), accepted by EPJC;
[3] ATLAS Collaboration, *Eur.Phys.J.*, **C71** (2011) 1630,
ATLAS Collaboration, ATLAS-CONF-2011-011, http://cdsweb.cern.ch/record/1334563;
[4] ATLAS Collaboration, *Phys. Rev. D*, **85** (2012) 072004;
[5] K. Nakamura *et. al.*,*J. Phys. G*, **37** (2010) 075021;
[6] ATLAS Collaboration,
http://atlas.web.cern.ch/Atlas/GROUPS/PHYSICS/PAPERS/STDM-2011-06;
[7] ATLAS Collaboration, arXiv:1203.4051 [hep-ph] (2012), accepted by PRL;
[8] HERAFitter, `http://projects.hepforge.org/herafitter`.
[9] H.-L. Lai *et. al.*,*Phys. Rev. D*, **82** (2010) 074024;
[10] ATLAS Collaboration,
http://atlas.web.cern.ch/Atlas/GROUPS/PHYSICS/PAPERS/STDM-2011-43;
[11] ATLAS Collaboration, *Phys. Lett. B*, **707** (2012) 418;
[12] ATLAS Collaboration, *Phys. Lett. B*, **706** (2012) 295;
[13] ATLAS Collaboration, *Eur. Phys. J*, **C72** (2012) 2001;
[14] ATLAS Collaboration, *Phys. Lett. B*, **712** (2012) 289;
[15] ATLAS Collaboration, *Phys. Lett. B*, **709** (2012) 341;
[16] ATLAS Collaboration, *Phys. Rev. Lett.*, **108** (2012) 041804.